REPORT DOCUMENTATION PAGE

Form Approved
OMB NO. 0704-0188

1. AGENCY USE ONLY (Leave Blank)	2. REPORT DATE 16 June 2006	3. REPORT TYPE AND DATES COVERED Final, 28 February 2005 through 27 April 2006

4. TITLE AND SUBTITLE
Electrodynamic Aerosol Concentrating And Sampling

5. FUNDING NUMBERS
W911NF-05-C-0037

6. AUTHOR(S)
David S. Ensor and Philip A. Lawless

7. PERFORMING ORGANIZATION NAME(S) AND ADDRESS(ES)
RTI International
POB 12194
Research Triangle Park, NC 27709

8. PERFORMING ORGANIZATION REPORT NUMBER 0209565

9. SPONSORING / MONITORING AGENCY NAME(S) AND ADDRESS(ES)
U. S. Army Research Office
P.O. Box 12211
Research Triangle Park, NC 27709-2211

10. SPONSORING / MONITORING AGENCY REPORT NUMBER
47224.1-CH-CDP

11. SUPPLEMENTARY NOTES
The views, opinions and/or findings contained in this report are those of the author(s) and should not be construed as an official Department of the Army position, policy or decision, unless so designated by other documentation.

12 a. DISTRIBUTION / AVAILABILITY STATEMENT
Approved for public release; distribution unlimited.

12 b. DISTRIBUTION CODE
.

13. ABSTRACT (Maximum 200 words)

The objective was to develop an electrodynamic bioaerosol concentrator with low energy requirements. A new low loss charger was developed for large particles. The charged particles were introduced into the quadrupole energized up to 10 kV AC in a flowing gas stream of about 0.8 Lpm. The 3 micron diameter polystyrene latex particles were focused to the center line of the electrodes. A He-Ne laser was aligned with the center line of the electrodes and the focusing was observed from scattered light. A fundamental model was developed and compared to the experimental conditions. The particle charge and residence time were observed to be most important. Frequency was found to be insignificant. The best application of this device might be to focus bioaerosol into the focal point of an optical particle detection system.

14. SUBJECT TERMS
Bioaerosol
Aerosol charging
Quadrupole
Concentrating and focusing

15. NUMBER OF PAGES
37

16. PRICE CODE

17. SECURITY CLASSIFICATION OR REPORT	18. SECURITY CLASSIFICATION ON THIS PAGE	19. SECURITY CLASSIFICATION OF ABSTRACT	20. LIMITATION OF ABSTRACT
UNCLASSIFIED	**UNCLASSIFIED**	**UNCLASSIFIED**	**UL**

NSN 7540-01-280-5500 **Standard Form 298 (Rev.2-89)**
Prescribed by ANSI Std. 239-18 298-102

ELECTRODYNAMIC AEROSOL CONCENTRATING AND SAMPLING

Prepared for
Contracting Officer's Representative:
Stephen Lee
US Army Research Office
Attn: AMSRD-ARL-RO-PC
PO Box 12211
Research Triangle Park, NC 27709-2211

Prepared by
David S. Ensor and Philip A. Lawless
Research Triangle Institute
PO Box 12194
Research Triangle Park, NC 27709-2194

Sponsored by
US Army Research Office
Contract No: W911NF-05-C-0037

RTI Contract No. 0209565

June 16, 2006

Foreword

This project was proposed as a two-year program to develop a concept to concentrate aerosol with electrodynamic forces. The milestones planned at the end of the first year were 1) development of a low loss particle charger and 2) a theoretical model. The milestones planned at the end of the second year were 1) development the quadrupole electrode section and 2) interfacing the quadrupole electrodes to the previously developed charger and obtaining extensive characterization data.

Fortuitously, we decided to conduct the research in parallel instead of in sequence because the second year was not funded. In the first year, the planned milestones for year one were completed. In addition, the first milestone for the year two and part of the second milestone were completed as well. The characterization data and additional refinements of the system were not completed.

The project was successful. As described in the following final report, 3μm polystyrene latex (PSL) particles were focused and concentrated. A novel way of illuminating the experimental apparatus with a laser beam down the centerline proved to be extremely useful in conducting the developmental experiments.

Table of Contents

Illustrations and Tables

Section I. Statement of the Problem Studied

In this section, we summarize the research objectives, background and technical approach. The interest in electrodynamics is the potential for a low-energy and compact bioaerosol concentrating device.

A. Research Objective

The objective of this research is to develop a new low energy method to concentrate bioaerosol to enhance subsequent detector sensitivity. This work involved developing a new low-loss particle charger. The charged aerosol was passed through quadrupole electrodes energized with about 4 kV AC where the voltage gradient forces the particle to the center line. The concentrated aerosol can be measured directly by focusing a light source at the focused aerosol to measure light scattering and/or fluorescence or sampled with a probe.

B. Background

Because the concentration of threat agents in ambient air would be low outside of the core of the release plume, it is desirable to sample a large volume of air and concentrate the particles of interest into a flowing stream that can be delivered to a detector for analysis. Concentration implies that the particles must be moved across flow streamlines, with most of the flow being discarded after the particles have been separated. This movement of particles can be accomplished by using inertial forces associated with changing the air flow direction or by applying external forces that affect the particles without affecting the air flow directly.

Inertial separation is used in impactors, particularly virtual impactors, in cyclones, and in aerodynamic focusing lenses. Types of external forces that can be used are electrostatic (moving charged particles with electric fields), magnetic (but only for magnetically susceptible particles), acoustic, and gravitational. Electrical forces are frequently used because they are strong compared with other forces and require relatively little energy to affect separations.

1. Aerosol Concentrating

Traditional impactors collect particles on a hard surface or into a liquid for later analyses. Virtual impactors separate particles from the major flow stream, yet retain particles in the airborne state, essentially concentrating them in-flow [Marple and Chien, 1980]. Similar to particle beams, virtual impactors have been utilized as sampling inlets for single particle counters/sizers [Keskinen *et al*., 1987; Liebhaber *et al*., 1991]. Also, virtual impactors have been implemented in toxicological research for inhalation studies [Sioutas *et al*., 1997; Kim *et al*., 2001], as well as being designed for bioaerosol sampling and detection [Romay *et al*., 2002]. Due to the greater inertia of larger particles, virtual impactors typically are more effective with larger particles (those larger than ~1 μm in diameter). In the sub-micrometer size ranges, special considerations in impactor design must be considered because small particles follow the flow stream more closely than do larger particles [Kim *et al*., 2000] and require significant pressure drop for operation. Typically, particle concentrating does not occur broadly over all particle size but typically over a size spectrum, typically ranging from one to two orders of magnitude.

2. Electrodynamic Particle Focusing

Electrodynamic focusing is a type of electrical concentration that moves electrically charged particles across flow lines towards a region where the net electrical force is zero. [Masuda and Fujibayshi, 1970; Berg, 1970; Periasamy *et al*., 1995]. Once the particles reach that location, there are in principal no forces to move them away and the volume they then occupy is much smaller than the original volume of air from which they came.

Fundamental principles prevent such localization with static electrical fields (not varying in time), but time-varying fields can be arranged to produce a net electrical field that does produce the localization. Because the fields must vary, the focusing is termed "electrodynamic."

A geometry that works particularly well is the linear quadrupole. It consists of four parallel conductive rods arranged with their centers on a square, as shown in Figure 1. The air flow is introduced along its long axis. The rods are connected to the voltage supply as diagonal pairs, so that the maximum electrical fields occur in the shortest gaps between the rods. The effective time-varying field near the quadrupole center axis varies as the square of the distance from the central axis. This effectively places the particles in a simple harmonic potential well; once they settle into the center of the well, there is no net force on them.

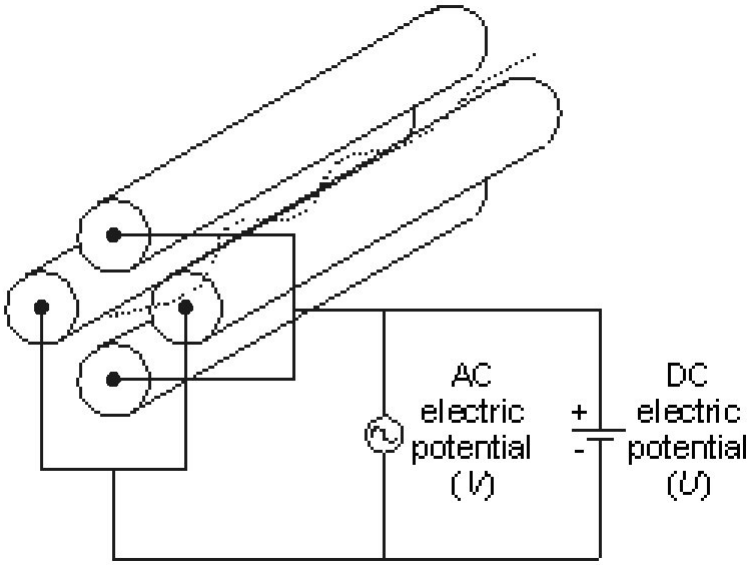

Figure 1. Schematic diagram of a linear quadrupole

In principle, all spherical particles can be aligned in the direction of flow with their centers on the central axis of the quadrupole. The concentration that results is from the original air volume down to a cylinder of dimensions equal to the particle diameter and average spacing between particles. It is like a multilane highway with traffic that merges into a single lane.

Most of the theoretical work on electrical quadrupoles deals with mass spectrometry where the quadrupole allows specific charge/mass ratios to pass through and all others to be rejected. In a sense, the mass spectrometer quadrupole is a resonant selective gate, with little or no attention paid to the focusing properties. In fact, with any harmonic oscillator, there must be some damping of the motion to allow the particle to settle into the minimum potential location. For airborne particles, the viscosity of the gas provides the damping. The theory for the vacuum

quadrupole must be extended to include viscous damping forces to be applicable to the electrodynamic focusing quadrupole.

In previous work, Ensor (2002) derived the equations of motion with the damping included as part of an attempt to obtain electrodynamic focusing of ultrafine particles

C. Technical Approach

The extreme focusing properties of the electrodynamic quadrupole pose some challenges in its use. For one thing, sampling of the focused aerosol stream will cause unwanted dilution by pulling air into the sampling line along with the particles. For another, the focused particles are expected to be highly charged. The presence of charge would accentuate losses in sampling lines leading to other analysis instruments. Another unwanted indirect effect is a time delay between the exit from the quadrupole and the point of analysis.

As a result, it is thought that the most likely application of electrodynamic focusing is as a localizer for an optical instrument. That is, the particle beam-like output from the quadrupole should be delivered directly to the active optical volume of an instrument, such as a laser-fluorescence device. In this way, the charges on the particles are made irrelevant and the highest concentrations of the quadrupole are effectively used.

This optical utilization suggested that most of the operating parameters could be characterized by simply observing the particle focusing directly, using a laser illuminator (laser plus beam expander) to view the whole particle path from the inlet of the charger all the way to the outlet of the quadrupole.

For this approach to work, particles of a proper size to be visible in the laser beam were need. Fortunately, PSL (polystyrene latex) particles in the range 3 – 5 μm in diameter are highly visible in an intense beam, similar in size to spores and bacteria of interest, and of a size that the models suggest can be well-focused.

The other important aspect of quadrupole focusing is the development of an adequate particle charging system. Aerosol charging has a long history, but the quadrupole application poses some interesting challenges. It is desired to place high charges on the individual particles to give the quadrupole fields good leverage for moving the particles. On the other hand, it is desired that few particles be lost in the charging process, lest the concentrating capabilities of the quadrupole be crippled before they can operate.

In the laboratory setting with nebulized particles such as PSL, induction charging of the liquid spray can be very effective. However, with the ultimate goal being concentration of ambient aerosol particles, it was thought that the efforts should be concentrated on charging of airborne particles.

Traditionally, the charging of small aerosol particles (diameters less than about 0.5 μm in diameter) is described as a diffusion process that is not strongly influenced by externally applied fields. Also, charging of large particles (larger than about 10 μm in diameter) is described as a field process, with the externally applied field driving ions to the particle surface. In reality, both mechanisms occur for all particle sizes, but one or the other dominates charging in the extremes. In the particle range between 0.5 and 10 μm, both mechanisms are important. Fortunately, a sound charging theory exists for the full range (Lawless, 1996) and is easily applied.

Charging in the presence of an electric field gives the particles maximum charge, but the field tends to drive the particles to the walls of the charger. It is possible to minimize the collection of the particles by increasing the gas flow velocity, by introducing a boundary flow of

air through a porous wall in the charger, or by using alternating current fields to reverse the particle motion periodically.

Increased flow velocity reduces the exposure time of the particles to the ions, and so partially defeats the goal of delivery high values of charge. The porous wall flow approach avoids that problem, but adds additional air to the incoming particle-laden air. This provides a potential dilution before any concentration can take place, although careful design might overcome any dilution effect. The alternating field technique seemed to be the most promising approach and has literature citations to support it (Jaworek and Krupa, 1989; Dalley, et al., 2005; Biskos, et al., 2005). Bidirectional ionic charging does also improve the maximum charge that can be given to highly insulating particles, although most ambient aerosols would not be of this type.

Consequently, the program proceeded along the following general path. An initial modeling effort indicated that particles several micrometers in diameter would be focused at AC frequencies of a few tens of Hz if they could be highly charged and the quadrupole fields were as large as possible. Dual experimental investigations for the charger section and for the quadrupole section were undertaken, with most of the work devoted to the charger. As each experimental device was produced, various tests were performed to indicate its operation. When a near-final configuration for both charger and quadrupole were reached, the whole device was assembled for testing and refinements continued to be made. Although the final configuration may still not be optimal, it does produce the focusing that was the goal of the program.

Section II. Summary of the Most Important Results

In this section, we summarize the most important results for the theory/modeling efforts, for the chargers and quadrupoles separately and together, with photographs and simulations of the experiments.

A. Theory and Modeling

There are two theories involved in this work, one for the charging and one for the electrodynamic focusing. Both theories were implemented as models during the program, basically spreadsheet versions that incorporated the essentials of the theories and allowed results to be quickly calculated and displayed. The theories were not developed under this program, but the models applying them were. Nonetheless, some discussion of the theories will be useful in understanding how the models worked.

1. Charging Theory

The theory developed by Lawless(1976) relates particle charge, applied electric field, and ionic charging current in terms of dimensionless quantities. The charging rate is expressed in terms of a field-charging rate and a diffusion charging rate, both perfectly equivalent to the classical descriptions of these terms. However, what distinguishes the Lawless theory from other charging theories is the combination of the terms.

The charging rate in the theory is given by:

$$\frac{d\nu}{d\tau} = F(\nu, w) + f(w)Be(0) \quad , \qquad 0 \le \nu \le 3w$$

$$\frac{d\nu}{d\tau} = f(w)Be(\nu - 3w) \quad , \qquad \nu > 3w \tag{1}$$

where ν is a dimensionless charge, τ is a dimensionless charging time, w is a dimensionless electric field, *F(v, w)* is the field charging function, *Be(x)* is the diffusion charging function (also called the Bernoulli function), and f(w) is the fraction of the particle surface area available for diffusion charging. These equations say that both field and diffusion charging (at its maximum rate) take place on the particle surface until the field charging limit is reached (ν = 3w), whereupon diffusion charging continues indefinitely from that maximum rate. The area function f(w) defines the relative contributions of the diffusion term in relation to the field term and is the factor that smoothly transfers the charging regime from one mechanism to the other.

The dimensionless parameters are complicated, but need only be evaluated once in the spreadsheet implementation. The charge is obtained by integrating Equation 1 with a simple time-step summation. Since the charging conditions are not precisely known, this is adequate for most simulations.

One of the important parameters for charger modeling is the ionic current density (current per unit area), that determines the overall dimensionless charging time. The usual range for current density in corona devices is 10^{-5} to 10^{-4} A/m^2 and the dimensionless charging times rarely exceed 300. These typical parameters were used as inputs for the charging model to estimate the values of charge that could be expected.

After we experienced difficulties delivering charged particles to the quadrupole section, an approximate measurement of the charging current was made to allow a computation of the current density. The surprising result was that the current density was easily as much as $2.5 \times 10^{-3}/m^2$ with a corresponding dimensionless time of 12000. It could be driven an order of magnitude higher. The charging conditions were so good that most of the particles were being captured before leaving the charger, even with the ac fields attempting to prevent this. The following Table 1 shows some of the relevant charging conditions.

Table 1. Charging conditions

Parameter	Typical	3 μm PSL	5 μm PSL
Current Density	5×10^{-4} A/m^2	2.5×10^{-3} A/m^2	2.5×10^{-3} A/m^2
Dimensionless Time	300	12000	12000
Dimensionless Field	1-10	0.7	1.2
Dimensionless Charge	7	13.8	15
Number of electrons	62	360	650

When the charge on the particles is known, the effect of the ac fields for preventing particle collection can be evaluated. The amplitude of motion of individual particles is calculated to be much less than one millimeter at 60 Hz.

2. Particle Motion in a Quadrupole

Referring to Figure 1 for orientation using an angular coordinate system around the centerline axis of the electrodes, the equations of motion including aerodynamic drag are summarized here.

$$\frac{du_p^*}{dt^*} = -\alpha u_p^* - \beta n r^{*n-1}\left(\frac{U}{V} + \cos\left(2t^* + \phi_i\right)\right)\cos(n-1)\theta \tag{2}$$

$$\frac{dv_p^*}{dt^*} = -\alpha v_p^* + \beta n r^{*n-1}\left(\frac{U}{V} + \cos\left(2t^* + \phi_i\right)\right)\sin(n-1)\theta \tag{3}$$

where the initial dimensionless phase difference is $\varphi_i = \omega t_0$. The dimensionless parameters are:

$$\alpha = \frac{6\pi\mu d_p}{m_p C_C \omega} = \frac{2}{\tau\omega} \tag{4}$$

$$\beta = \frac{4q_p V}{m_p \omega^2 r_0^2} \tag{5}$$

$$u_p^* = \frac{2u_p}{\omega r_0} \tag{6}$$

$$v_p^* = \frac{2v_p}{\omega r_0} \tag{7}$$

$$t^* = \frac{\omega t}{2} \tag{8}$$

$$r^* = \frac{r}{r_0} \tag{9}$$

$$\tau = \frac{m_p C_C}{3\pi\mu d_p} = \frac{\rho_p d_p^2 C_C}{18\mu} \tag{10}$$

$$C_C = 1 + \frac{\lambda}{d_p}\left[2.514 + 0.800\exp\left(-0.55\frac{d_p}{\lambda}\right)\right] \tag{11}$$

where the variables are defined as follows:

C_c	Cunningham correction factor (for particle slip in a flowing stream)
d_p	particle diameter
f	frequency
m_p	particle mass
n	number of pole pairs (= 2 for quadrupole)
r	radial position of charged particle
r_0	radius of quadrupole from centerline to surface of electrodes
t	time
U	DC potential
u_p	x-axis particle velocity
q_p	particle charge
Vac	voltage amplitude
v_p	y-axis particle velocity
ρ_p	particle density
λ	mean free path of gas molecule
μ	gas viscosity
ω	angular frequency ($2\pi f$)

By fixing the number of pole pairs at 2 for the quadrupole and omitting the phase angle φ in the cosine terms, the equations are further simplified. The angle θ represents the azimuthal starting point for the particle trajectory, with θ = 0 or θ = 90 corresponding to locations along the lines joining opposite pole.

The spreadsheet implementation involves a Visual Basic module for Runge-Kutta calculations of the particle trajectory, with graphical and tabular presentations of the results. A particularly useful presentation is shown in Figure 2, with the trajectory collapsed into a projected x-y plane down the axis of the quadrupole. This is essentially what would be seen if a particle were observed along the z-axis. The surfaces of the rods are located at (1, 0) and (0, 1), so that trajectories exceeding those limits represent particles that are captured.

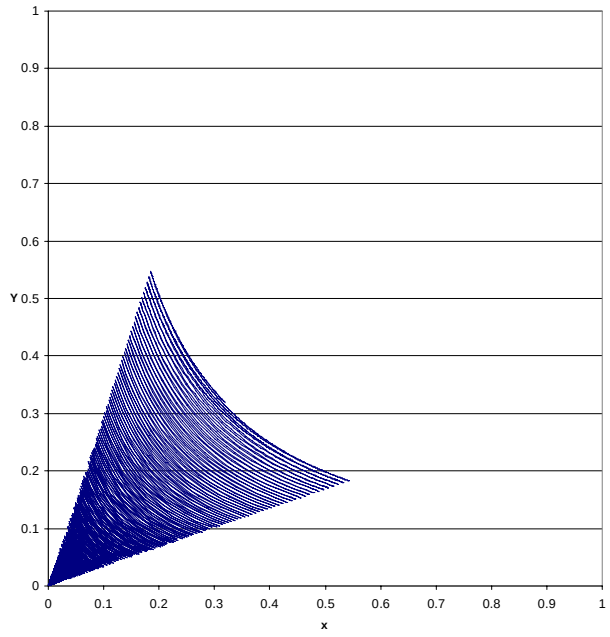

This calculation is for a 5 µm particle released at an azimuthal angle of 45 degrees 0.5 cm from the centerline of the quadrupole. The trajectory takes 9 seconds to approach the centerline to within 10^{-5} cm. After 4 seconds, it was within 0.01 cm.

Figure 2. Calculated trajectory projected on x-y plane

The model has revealed the following important points about the operation of the electrodynamic focusing:

1. The approach towards the centerline follows an exponential law. Calculating the logarithmic decrement allows the time to approach to within any arbitrary distance to be estimated very well.

2. The approach rate is a strong function of the particle mass. This has been verified in the model by changing the density of the particle while leaving all other parameters constant.

3. The frequency of the quadrupole voltage affects the motion, with lower frequencies giving larger excursions and faster focusing. However, in practical terms, 60 Hz from the power mains is not far from optimal.

These three model results imply that particle inertia allows the particle to cross electric field lines as it approaches the center axis. Without inertia, the viscous damping of the gas would still occur, but the particle would move no nearer the center as it follows the ac cycle.

As a result of this initial study, it appears that the electrodynamic focusing may become too slow for biological particles (specific gravity near 1) at a diameter slightly less than 1 µm. This is not a problem that can be overcome with only increased charge on the particles. The residence time must be increased by increasing electrode length or by reducing airflow.

One other aspect of the model has proven useful. By using the logarithmic decrement from the detailed calculations, it is possible to estimate a velocity of approach of the particle to the centerline. Because the particle does not overshoot the centerline (at these particle mass

values), the velocity becomes very low near the center. Any small air currents across the center axis can be sufficient to prevent complete focusing. Other phenomena may have the same effect.

B. Experimental Approach

The program effort initially addressed the charger configuration, and then the quadrupole configuration. Three types of charges were evaluated, with the final configuration being a variant of the second one tried. Two quadrupoles were used, one that had been built as part of the previous effort (Ensor, 2002), and a second that was designed to overcome the deficiencies of the first.

1. Chargers.

Three types of corona chargers were tried. Corona provides high ionic densities suitable for both diffusion and field charging conditions. Other types of ion generation were not considered.

Corona is generated when a small diameter electrode is connected to a high voltage with respect to a larger diameter collecting surface. The corona is initiated by random ions (from cosmic rays) but is sustained by ionic and photonic feedback. To provide usable ions for charging, the opposite collecting surface needs to be porous to some extent to allow ions to pass through.

Charger 1. The first charger is shown in Figure 3. It is called a Hewitt-type charger, after the author who first used it.

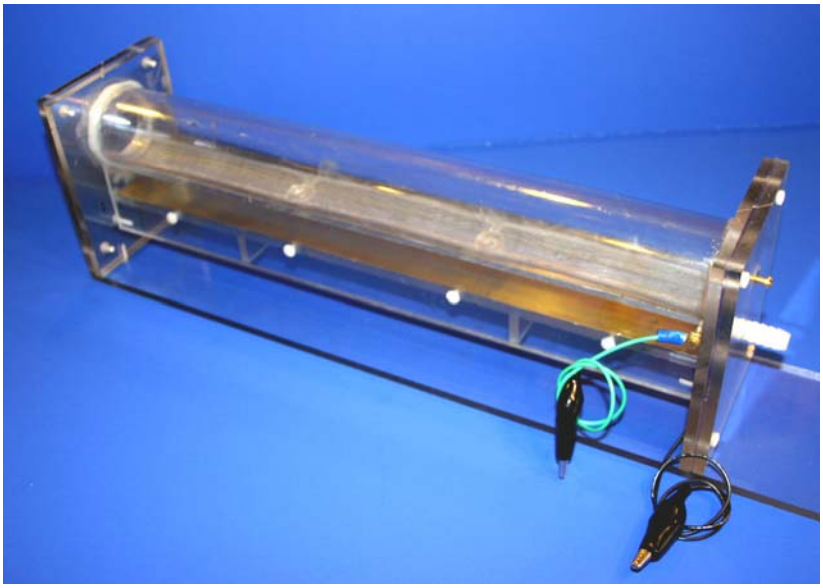

Figure 3. Hewitt type corona charger with central wire, porous wire counter electrode and flat-plate ac electrode

The fine central wire (76 μm diameter tungsten) was expected to provide a very uniform corona with positive tenderization. The current to the collector electrode (a 45 percent open stainless steel mesh) would be easily calculated, and the ions would be available for charging in the ac field region between the flat plate and the collector electrode.

The charger worked as predicted electrically. Its current was easily controlled and it provided a good flow of ions to the flat plate. However, it failed to prevent deposition of particles. The charger was challenged with 1.03 µm polystyrene latex (PSL) at a flow rate of 2 Lpm with a concentration of about 250 particles/cm^3 as measured by an optical particle counter. When any detectable amount of corona current flowed, all particles were lost, even when the field plate was energized up to 700 VAC at frequencies from 90 to 600 Hz.

Without thoroughly analyzing the charger, we think two problems contributed to the losses. First, the ac field geometry would tend to move particles towards the sides of the flow channel. Second, the ion movement produces a corona wind wherein the motion of the ions is partially transferred to the gas. In this geometry, the corona wind would also be expected to push the particles towards the sides of the flow channel. The corona charger of Biskos et al.(2005) would not have these limitations because it has a completely symmetric cylindrical arrangement. We would have tried a Biskos-type charger eventually if other devices had not worked.

Charger 2. Since a separate charger had failed to work, it was thought that a charger inside the quadrupole might result in lower losses. Figure 4 shows a fine hypodermic needle used as a corona wire within the first quadrupole. The quadrupole electrodes would serve as the collecting surfaces. Since the charging would be within the quadrupole, no AC control of losses would be needed.

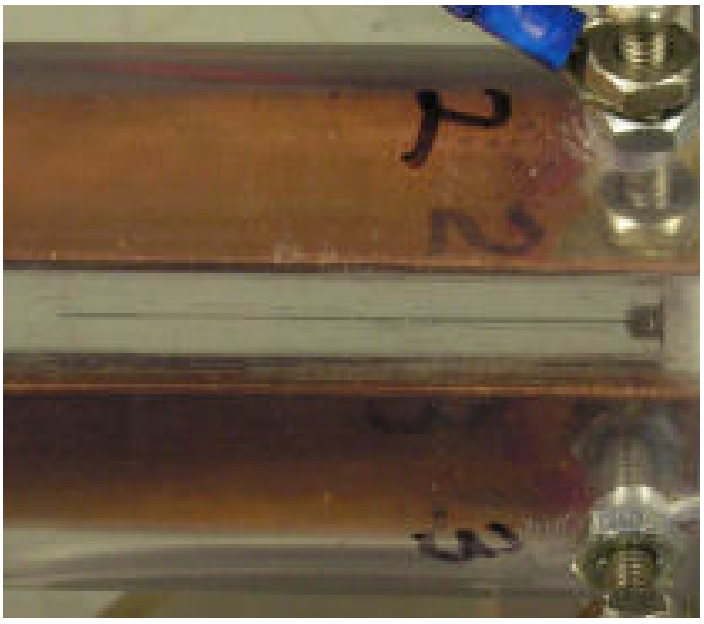

Figure 4. Corona needle inserted into quadrupole.

This arrangement did work as a corona device. The flow of DC current to the quad electrodes revealed that the transformer energizing the quadrupole had an open winding, even though there was enough capacitive coupling to provide the desired AC voltage. However, we quickly realized that most of the DC current would flow along the shortest paths to the electrodes, leaving much of the gas flow without sufficient ions for effective charging. The arrangement would also prove difficult to vary the charging and quadrupole conditions for optimal results.

Several days of testing with the optical counter and a movable sampling probe to detect focusing verified these problems. It was difficult to measure the DC ionic currents in the presence of the AC quadrupole voltages. Although particle charging did seem to be taking place, as evidenced by particle reductions, no detectable focusing was observed. This geometry might prove useful in the future to make a more compact unit, but careful optimization would be required.

Charger 3. While little progress was being made with the second charger, a third charger was under construction, based on the designs in Jaworek and Krupa (1989) and in Dalley, et al. (2005). This charger is shown in Figure 5. It uses pin electrodes arranged to allow most of the ions to pass into a central region. The left and right sets of pins are energized on opposite half cycles of the supply voltage, with the result that ions flow towards particles in the central region from two directions.

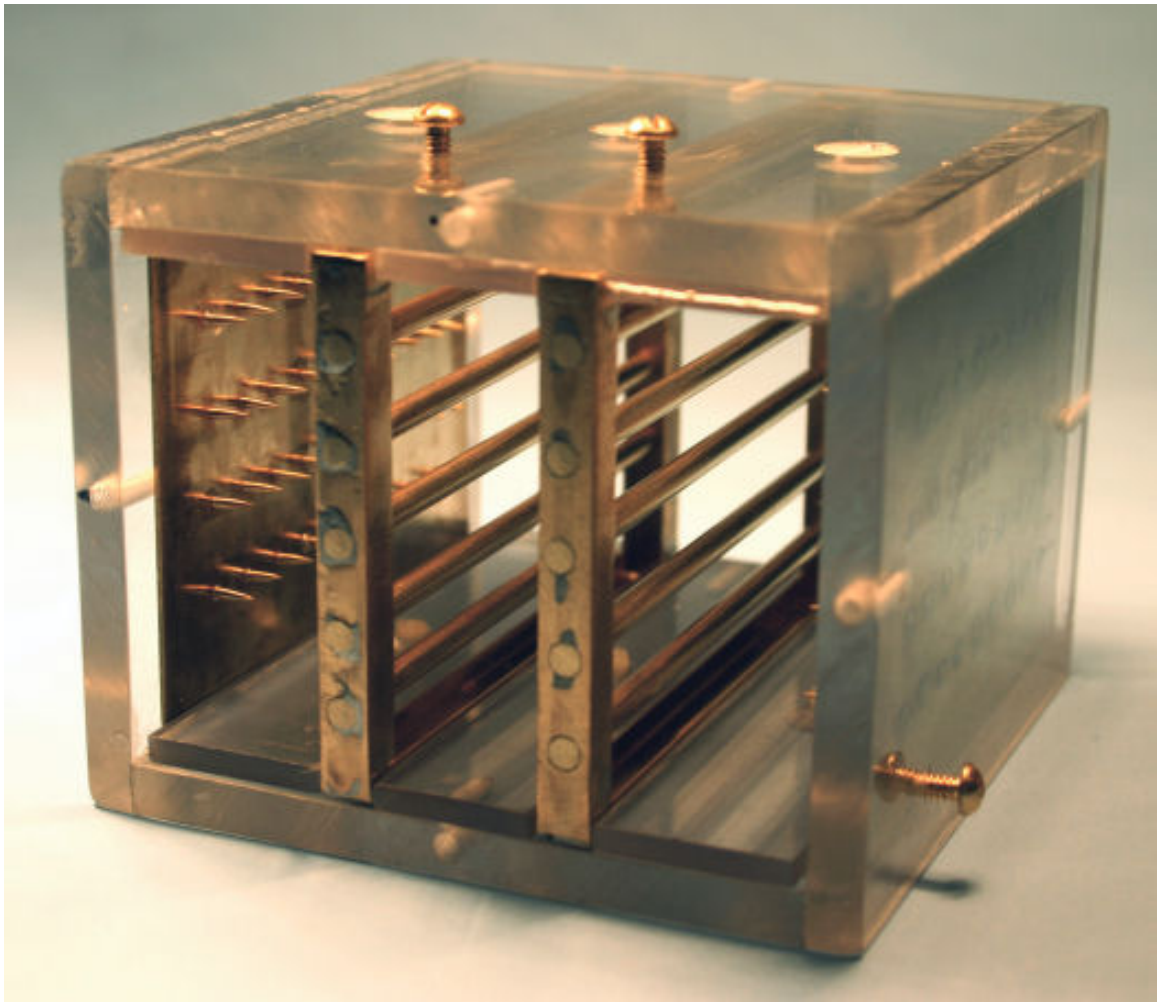

Figure 5. Dual direction pin-plate charger. Particles would flow parallel to the rods

The pins in this charger were not expected to carry equal amounts of current. It is very difficult to get the corona on adjacent electrodes to start at the same voltage. Negative polarity was used

for the corona, because the negative ions tend to spread at a wide angle and remain unipolar, whereas positive polarity tends to form narrow streamers that are almost electrically neutral.

This charger underwent several evolutionary changes, which will be described later. All of its usage was with the second quadrupole design and so is more easily discussed in that context.

2. Quadrupoles

Two quadrupole designs were tried. The initial concept was that quadrupole precision was not particularly critical in this application, as distinct from mass spectrometer uses. This was based on anecdotal stories of successful 3-dimensional quadrupole particle traps being constructed out of two quarters and a loop of wire. Lack of success led us to question this assumption.

Quadrupole 1. The first quadrupole was based on sections of copper pipe that had been previously built. Figure 6 shows most of its aspects.

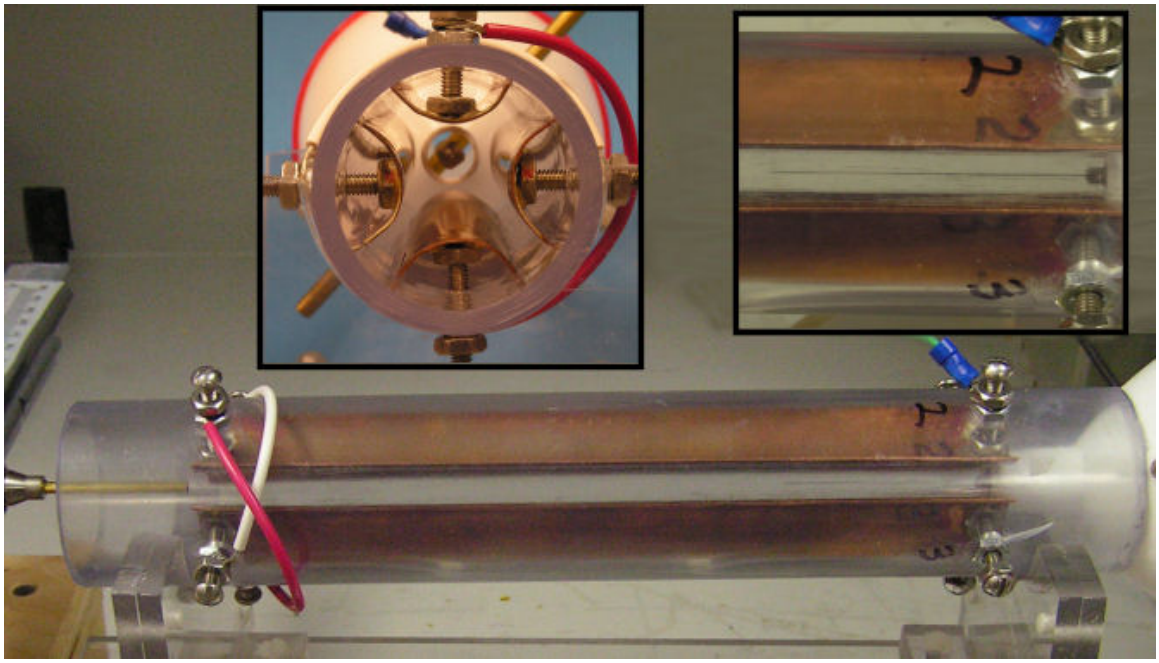

Figure 6. Sectional quadrupole in round pipe. The sampling probe is shown at the left end.

This quadrupole was originally built to better control the flow of gas between the electrodes. The theory of quadrupole focusing assumes the electrodes are hyperbolic surfaces that extend to infinity, whereas the round rods give a good approximation of the same electric field configuration when spaced at a critical fraction (0.872) of their diameter (Denison, 1971). The copper pipe sections were carefully expanded to better approximate hyperbolas.

It is shown here with the inner needle corona electrode in place. Once it was determined that the needle was not working, it was removed. Before the quadrupole could be used with another charger, a test showed that the maximum voltage that could be applied between electrodes was about 3.5 kV, limited by sparking at the sharp edges of the cut pipe sections. Since the model had shown the advantages of maximizing the applied voltage, another quadrupole was designed.

Quadrupole 2. The second quadrupole was designed specifically to maximize the voltage that could be applied. It was constructed of aluminum rods with rounded ends. They were not perfectly spherical, but could have been made so if needed. The assembled rods were able to sustain 7.5 kVac RMS, which was the maximum voltage available.

More attention was also paid to spacing and alignment. Slab spacers of the proper thickness were inserted between electrodes as their mounting screws were tightened, and a plastic pipe of the proper diameter was used to set the interelectrode separations. The alignment tools also ensured parallelism. Figure 7 shows the second quadrupole.

The solid rods eliminate some of the flow problems, but the space between the rods and the surrounding box provided other flow paths.

End plates were attached with flow holes in the center and mounting holes along the top and bottom of the walls. At this stage, the method of viewing the particle beam was not certain and several mounting bolts were placed in unfavorable positions. Some of the plastic faces were also scratched in unfortunate locations.

The rods were numbered on each end to allow them to be replaced exactly if they needed to be removed.

Figure 7. Second quadrupole built with 2.54 cm diameter rods.

3. Full System

As the pieces of the project came together, the assemblage was determined. The modeling had indicated that particles of 3 to 10 µm should be used, so plans were made to deliver the particles to the quadrupole and charger vertically, avoiding gravitational losses and possible bending of trajectories. A high output nebulizer was first used, and a silica gel diffusion dryer was placed next in line. The third charger unit was mounted directly above the quadrupole section and closely coupled with it.

Frustration with the difficulty of detecting focusing with a sampling probe led to the concept of placing a laser light sheet at the outlet of the quadrupole so that a collapse of the particles into a small area could be visually detected. This configuration is shown in Figure 8. Overnight, it was recognized that axial illumination all the way up quadrupole into the charger would be even more beneficial.

The laser was remounted with a mirror to guide the beam upwards. A beam expander was installed to fill most of the interelectrode space. The resulting beam could be swept across the remaining gaps with mirror tilt screws.

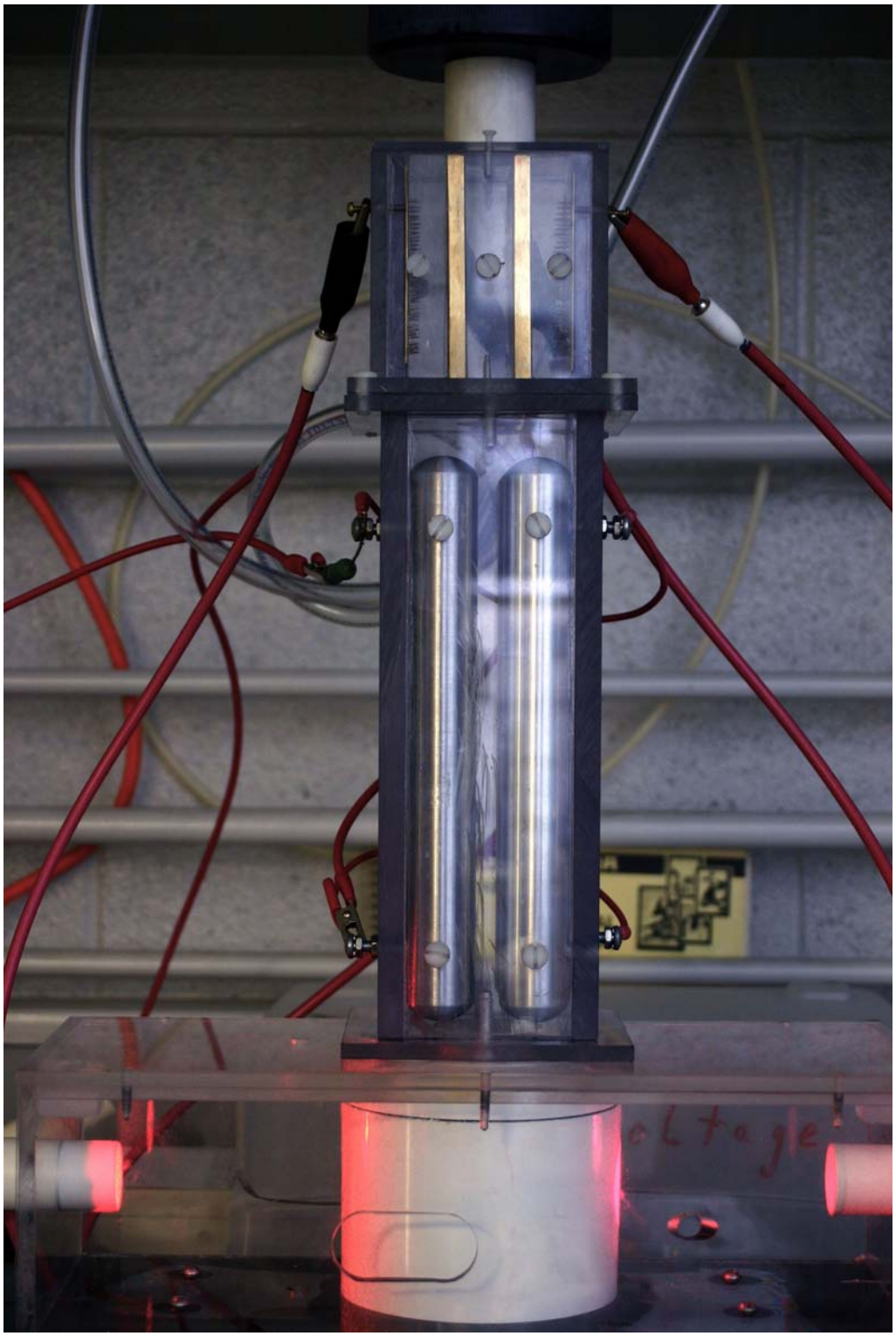

Figure 8. Quadrupole mounted below charger with provisions for illuminating the outlet.

The axial illumination became a key to understanding multiple aspects of the quadrupole-charger operation. By being able to see the charging volume, it was possible to detect the onset of charging and corona wind effects by the motions of particles. By being able to follow the particles all the way down through the quadrupole, convergence or lack of convergence to the centerline could be observed.

One effect that was first noted was that room air currents caused some deflection of the particles near the outlet of the quadrupole. Some outlet pipes (plastic) were added to decrease that influence, resulting in much more stable operation. It is likely that room air currents had influenced previous sampling measurements in other setups.

Some interesting phenomena involving particle motions were observed (described later), but focusing was not immediately observed. With the dual-directions charger, there was air swirling motions observed in the central space and it was very easy to stop any particles from entering the quadrupole. Eventually, by manipulating the charger conditions and the gas flow velocity, some focusing was obtained. It was not very reproducible, but it was a first success.

Charger 3a. The charger was addressed to improve its operation. As seen in Figure 5, there were multiple rows of pins. These seemed to contribute to the swirling motions without adding to the charging capabilities, since most of the particles passed only one row of pins in the direction of flow. The multiple rows were replaced with a single row on each side of the charger. At the same time, the rods were replaced with the open mesh stainless steel screen previously used in Charger 1. This change was made to help confine the gas flow to the central region and provide a more uniform electric field for the ac voltage on the grids. The new charger worked at least as well as the multi-row version, but still exhibited corona wind and uneven activation of the pins.

Charger 3b. Based on the assumption that uniform corona would be better than non-uniform corona, the pins were replaced with a single fine wire (on each side) with 25 μm indiameter. These were supported with one brass and one Nylon bolt to remove the influence of the brass plate. Such a plate makes the electric field more uniform but raises the corona onset voltage; with a wire electrode, it simple impedes the corona formation. The corona polarity was changed back to positive.

The charger seemed to work as intended, but the focusing was not easy to obtain. There was still much swirling in the central chamber.

Charger 3c. The current emitted into the chamber was further reduced by cutting a piece of brass foil to fit inside the mesh screen with an opening about 2 mm wide running just opposite the wire. (This was done on both sides of the charger.) This should have restricted the charging current to just the region occupied by the flowing particles. At this time, the second wire was simply disconnected and the current to its mesh grid was measured, without the ac voltage applied. The current that flowed amounted to about 1 μA, which is small. It was however, coming through a small slit opening and the current density was quite high, as much as 5 mA/m^2. Such current densities would lead to high particle charges (with collection) and corona wind effects. Further efforts reduce the current density were made.

Charger 3d. The brass foil with vertical slit was replaced with a plastic foil (Mylar) with a horizontal slit across the direction of flow. This was done on one side only. This slit did confine the charging region, with the particles showing little or no displacement until they reached the

level of the slit. The total current to the opposite mesh was still as high as before and the focusing was still poor. It was determined that the wire corona device simply reached a high current density with very little change of applied voltage. It was either off or on at a very high level; neither condition could deliver the charged particles for focusing.

Charger 3e. The final configuration was a flat-plate charger with a single pin located near the bottom of the charging chamber. The opposing AC deflection mesh was replaced with a brass plate slightly bent to help move the particles towards the exit opening. Its operation is not completely understood yet, but it seems to have a broad operating range.

C. Quadrupole System Operation

With the multiple changes of chargers, it seemed that the quadrupole would operate better after it was cleaned than if it had been in operation for a long time. One of the symptoms was this. Charged particles could be held in quadrupole by adjusting the flow rate to near zero. The particles seemed to be charged because 1) they vibrated when the field was on, but not when it was off and 2) they would maintain a fairly large spacing between themselves. Although they were moving in the field, they would not move to the centerline of the quadrupole.

Possible reasons for this behavior are:

1. Air currents that keep blowing the particles away from the centerline. This was been observed when the room air currents disturbed the outlet flow. It is hard to imagine sir currents with no particles in the air when the particles are almost motionless.

2. Charged particles near the centerline. This is known as space charge. Such particles would repel others, but should be visible. We have observed a related effect when many particles are being driven to the centerline. The concentration of charged particles prevents them all from focusing. Using the traffic analogy, too many cars on the road keep them from all being able to merge into one lane.

3. Charged surfaces on the quadrupole rods. The aluminum oxide on the surface of the rods could collect enough charge to displace particles away from the centerline. This might also be due to charged particles collected on the rod surfaces. Cleaning would remove such charges.

Item 3 was addressed by coating the aluminum rods with Aquadag, a graphite-based paint that was sprayed on the rod surfaces. The coating appears to be very smooth; it is electrically conductive; and particles are easily blown off the surface. The operation of the quadrupole seems to be improved by this change. In the future, the use of non-oxidizing metals for the quadrupole rods is recommended.

1. Focusing Results

A visual confirmation of focusing is hard to present quantitatively. Fortunately, some of the results have been successfully photographed and some of the more dynamic aspects have been captured on video tape.

2. Photographs of Aerosol Focusing

The following photographs in Figure 9 illustrate some of the best of the focusing results.

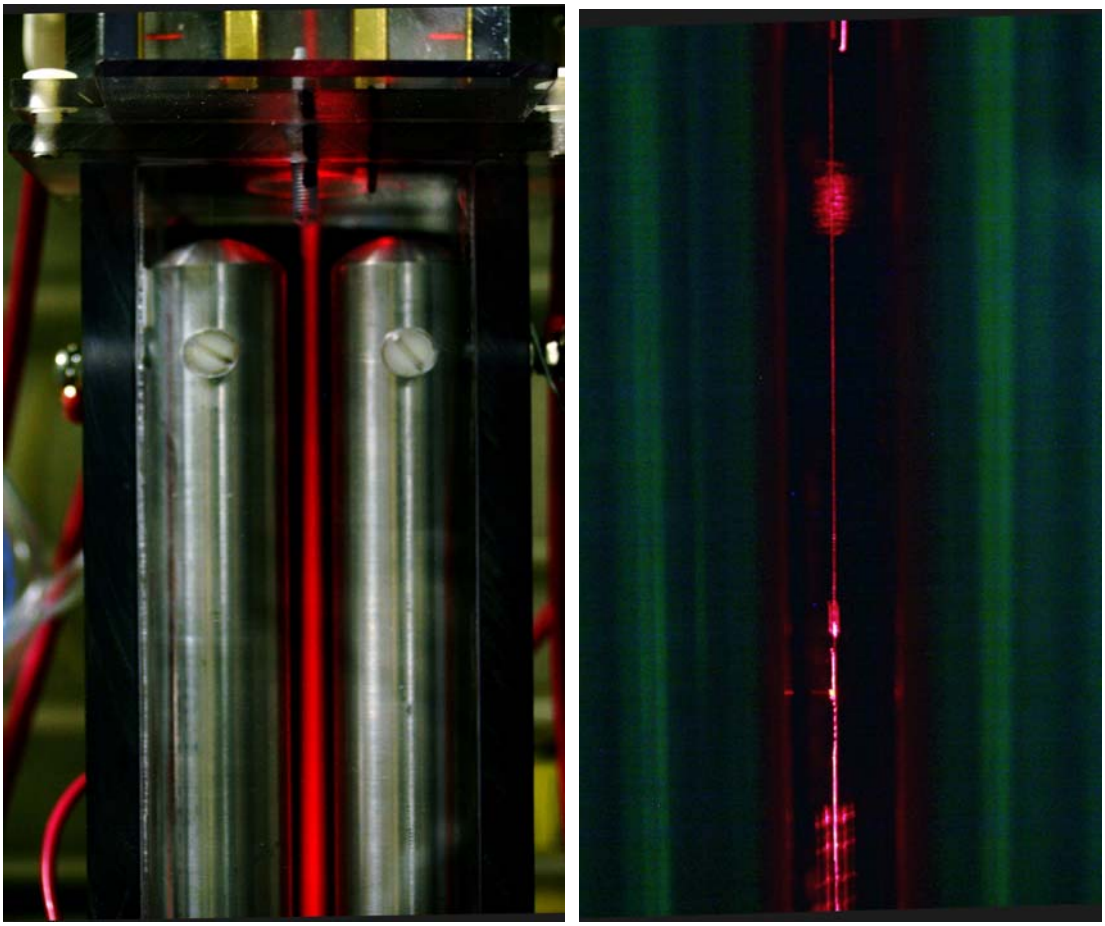

Figure 9. Left photo: unfocussed particles illuminated in the center of the quadrupole. The converging laser beam accounts for the apparent narrowing. Right: focused particles passing through particle groups oscillating in square patterns.

As mentioned before, other unusual effects have been observed within the powered quadrupole, often with even before turning on the charger. Sometimes large, bright particles with natural charge fall out of the drying column and can be caught in the quadrupole if the air flow is adjusted to a neutral value. The particles oscillate vigorously, but occasionally settle into a stable square or rhomboidal pattern of movement. The lines of motion follow the expected curvature of the field lines and so are not precise squares. The following photographs attempt to show some of these occurrences.

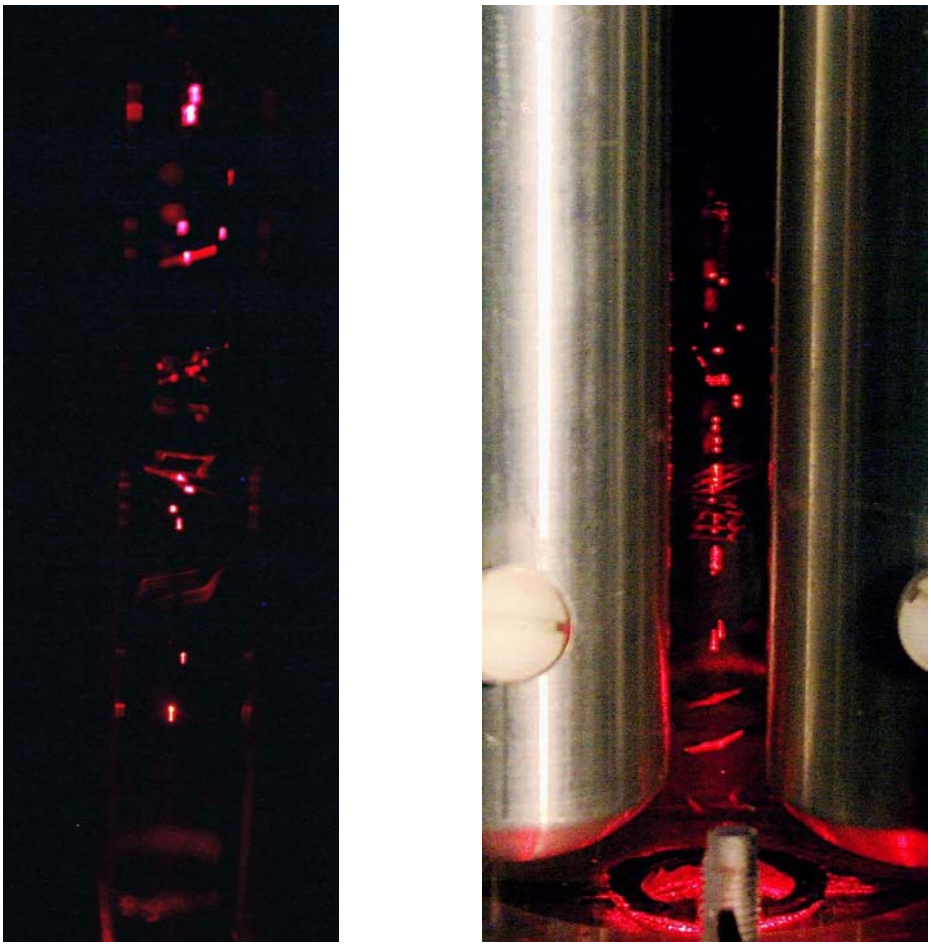

Figure 10. Groups of large oscillating particles, especially square patterns midway up each picture.

Because the patterns are large, open, and stable, it is suspected that two or more particles are involved, mutually repelling one another as they move in the electric fields. All of the normal quadrupole modeling does not allow particles to cross from one quadrupole sector into another. However, particles with sufficient inertia might be able to do so.

One square grouping was stable at the bottom of the quadrupole for tens of minutes. Other particles could be observed drifting through the center of the square (without any charge repulsion). As they drifted, they were imparted a definite rotary motion, as if being stirred by the particles moving around the square. This observation was the best confirming evidence of a continuous movement of particles around the square trajectory.

3. Other Observations

The one-pin charger operation is not well-understood. The fraction of charged particles is high and the loss of particles is low, both very desirable goals. However, when the charger is first turned on in the presence of particles, there is little visual evidence of corona and relatively little focusing of particles. After a few minutes of operation, the corona at the pin tip flashes brightly but irregularly, while the focusing becomes excellent. It seems as if some or most of the particles might be recycling though the charging zone before actually leaving the charger.

Particle space charge is observable when the particle concentration becomes too high. One manifestation is that some particles are well focused in the upper portion of the quadrupole but become unfocused further down as more and more try to reach the centerline. It is likely that a portion of the difficulties experienced with the experiments were due to space charge effects. When a 3-jet Collison nebulizer was used at it regular operating pressure of 16 psig, the particle concentration was 700,000 L^{-1}. Good focusing is now routinely obtained with 5000—15000 L^{-1}; this is obtained with a single-jet Collison nebulizer operating at 10 psig. Good focusing has been observed at a volumetric flow rate of 800 cm^3/s.

Suspensions of sterilized *Bacillus globigii* (Bg, provided by Dugway Proving Ground) and *B. thuringensis* (Bt) were each nebulized and sent through the system. The Bg showed definite focusing of large particles, with a large portion of smaller particles that were not focused. The sizing is based on the amount of light scattered. The Bt seemed to have fewer large particles, although the individual spores should be somewhat larger that those of Bg. There was some trend towards focusing, but also of space charge; both could be attributed to a smaller particle size.

It is not possible at this time to judge whether focusing of these spores is possible within a usable time. The model suggests times from hundreds to thousands of seconds, but the input parameters for the spores and charge state are poorly known.

4. Measurements

The particle concentrations for the PSL aerosols were measured using a MetOne Model 521 optical particle counter with thresholds set at 2 μm and 4 μm. Although the sizing calibration of the counter depends on the type of particle being measured, these nominal channels capture the mixture of 3 μm and 5 μm particles fairly well. Since the counter was used to determine change of concentration with one or another section turned on and off, the relative measurements are adequate. The counter samples at 2.8 Lpm and so almost always draws room air in with the sample. Checks of the room air concentration show that the correction for particles of these sizes is negligible.

The charger voltages are shown in Table 2 as both average DC values and peak DC values. The charger is energized with ½-wave rectified AC, with the mesh grid and the deflecting plate alternately connected to ground potential. The operating voltages are all in proportion to the DC pin voltage, which is monitored continuously.

Table 2. Charger operating voltages

Element	DC Voltage (kV)	Peak DC Voltage (kV)
Plate and pin	-3.13	-10.0
Mesh grid	-0.50	-0.85
Deflection plate	-1.48	-5.80

The presence of particles flowing through the charger does affect these voltages, making them difficult to measure due to the fluctuations.

The following measurements in Table 3 were taken with the quadrupole giving good focusing. It was not possible to be quantitative about the charged particle fraction, but the illumination showed only a small fraction of particles not being focused. The counter sampled the particles through a short piece of plastic tubing. Losses through the tubing were not characterized, nor was the sampling efficiency. For the most part, the on/off characterizations make this unimportant, although charge is expected to be a factor contributing to the losses. The delivery flow rate for these measurements was 0.8 Lpm.

Table 3. Outlet PSL particle concentrations (ppL)

Condition	> 2 µm	> 4 µm
Dryer outlet	21000	6800
Charger off ; Quad on	16300	4050
Charger on ; Quad off	11500	2360
Charger on ; Quad on	10400	2800
Charger transmission fraction	0.71	0.58
Quadrupole transmission fraction	0.90	0.70
System transmission fraction	0.50	0.41

These transmission fractions are very good. They imply that most of the particles of interest that enter the charger will be delivered in a focused beam at the outlet.

Average particle charge would be measured experimentally by collecting the particles in a Faraday cup and measuring either the current or charge accumulation rate. By knowing how many particles entered the cup, the average charge per particle could be computed. Unfortunately, the Faraday cup would have to be placed directly in the laser beam, or be made very small. Until that can be done, the best estimate of particle charge comes from the focusing itself.

The focusing during the 4-second transit time through the quadrupole at the flow rate of 0.8 Lpm was used to infer an average particle charge. The charge is about 7000 electrons per particle for both 3 µm and 5 µm particles, with slight differences in the final distance from the centerline. This amount of charge is larger than calculated by the charging theory by a factor of 2 to 5. The

only possible explanation for the large charge is that particles pass very close to the corona pin where the electric fields and charging currents are very high.

This explanation fits the observations about the corona turn-on and flashing behavior, but is not very satisfying. The direct measurement of particle charge would be preferable.

D. Parametric Simulations

With a working model, it is fruitful to examine the effects of changing various parameters within its frame work. The basic case for the parametric variation is as follows in Table 4.

Table 4. Base case parameters for simulation studies

Parameter	Value
Particle Diameter	5 μm
Density	1050 kg/m^3
Particle Charge	9750 electrons
Quadrupole Peak Voltage	10746
Frequency	60 Hz
Injection radius	0.70 cm
Injection azimuthal angle	45 degrees
Residence time	10 s

The density is that of PSL; the voltage and frequency are those used in the present system; the injection radius and angle give stable calculations (particles do not hit the electrodes); and the residence time corresponds roughly to the flow rates used. The calculation predicts the time for which the radial distance is 1 percent of the initial radius and the radius at the end of the residence time. Both are useful indicators of the aligning ability of the quadrupole.

For the base case, the 1 percent focusing occurs at 5.65 seconds (roughly halfway down the length of the quadrupole), and the final radius ratio is 2.87×10^{-4}, equivalent to 2.0 μm. This means the particle has settled to within its own radius of the centerline. Both of these parameters are ratios based on the injection radius; they do not show variations with the injection radius, although it should be clear that particles injected farther from the centerline do take longer to reach the centerline.

The first parameter to examine is that of density, because it has an unexpected effect on the focusing. Table 5 presents results for some realistic and extreme values.

Table 5. Density effects on focusing

Material	Density (kg/m^3)	Time to 1 % (s)	$R_{final}/R_{initial}$
Near neutral density bubbles[1]	70	41.4	0.33
Oleic acid	895	6.54	8.7×10^{-4}
Water	1000	5.91	4.1×10^{-4}
Polystyrene Latex (PSL)	1050	5.65	2.9×10^{-4}
Ammonium Sulfate	1769	3.46	1.6×10^{-6}
Carbon (fractal)	2000	3.45	3.1×10^{-7}
Aluminum oxide trihydrate	2420	2.94	$< 1 \times 10^{-7}$
Carbon (solid)	3500	2.94	$< 1 \times 10^{-7}$
Iron oxide (hematite)	5240	2.94	$< 1 \times 10^{-7}$

The density of the particle is important for reducing the time to focus in the range associated with bioaerosols, 1.0—1.5 g/cm^3. Most mineral aerosols would focus in a shorter time, as would metallic aerosols with even higher densities than shown. The reason for the saturation in focus time at the higher densities is not presently known. For small changes of density around the base case, the focus time changes in proportion to the change of density. This indicates that density has a first-order effect on the time to focus.

It is somewhat surprising that there is any density effect, since viscous drag is the major factor limiting the particle's velocity in the applied field. The drag should be in proportion to the particle diameter, but particle mass should have no effect. Mass would become important when the applied forces change rapidly with respect to the particle relaxation time (see Equation 10.) For the base case particle, the relaxation time is about 46 μs, meaning that much slower changes in forces should not exhibit a mass-dependent effect.

Varying the particle charge is a way to understand the importance of good charging conditions. This is done with a multiplying factor for the base case as shown in Table 6. The range of charges is not pushed to extremes because such charges may not be realizable.

[1] Lower density values produced collisions with the electrodes

Table 6. Particle charge effects on focusing

Multiplier	Charge (electrons)	Time to 1 % (s)	$R_{final}/R_{initial}$
0.5	4880	22.6	0.13
0.7	6830	11.5	1.8×10^{-2}
0.9	8780	6.97	1.3×10^{-3}
1.0	9750	5.65	2.9×10^{-4}
1.1	10700	4.67	5.2×10^{-5}
1.3	12700	3.34	1.0×10^{-6}
1.5	14600	2.94	$< 1 \times 10^{-7}$

For small changes in charge from the base case, the change in time is twice the change of charge, indicating a square dependence of focus time on the charge value. The time remains 2.94 seconds for higher values of charge, although collisions with the electrodes occur with somewhat larger increases of charge.

The peak electric field is close to its maximum value in the base case. Sparking between the electrodes occurs infrequently, but small amounts of contamination from collected particles can increase the rate of sparking. Varying the peak filed towards lower values allows this mode of degradation to be understood. Although a concentrator could be designed to have a safety margin in the applied field, doing so will result in a longer residence time to achieve the same focusing as shown in Table 7.

Table 7. Peak voltage effects on focusing

Multiplier	Peak voltage (V)	Time to 1 % (s)	$R_{final}/R_{initial}$
0.60	6447	15.7	5.3×10^{-2}
0.70	7522	11.5	1.8×10^{-2}
0.80	8597	8.82	5.4×10^{-3}
0.90	9672	6.97	1.4×10^{-3}
0.95	10210	6.26	6.4×10^{-4}
1.00	10746	5.65	2.9×10^{-4}

The change in focus time with a change in field is at twice the rate of change of the field (a five percent decrease in field increase the focus time by ten percent.) This indicates a square dependence of the focus time on the field and reemphasizes the importance of operating close to the sparking condition.

The frequency of the applied quadrupole voltage is expected to affect the focus time. If the frequency is very low, particles move continuously along the field lines until they collide with the electrodes, while very high frequencies would cause the particles to oscillate in position without moving towards the centerline. A wide range of practical frequencies is shown in Table 8.

Table 8. Frequency effects on focusing

Multiplier	Frequency (Hz)	Time to 1 % (s)	$R_{final}/R_{initial}$
0.7	42	5.24	1.5×10^{-4}
0.8	48	5.42	2.0×10^{-4}
0.9	54	5.55	2.5×10^{-4}
1.0	60	5.65	2.9×10^{-4}
1.5	90	5.89	4.0×10^{-4}
2.0	120	5.99	4.6×10^{-4}
3.0	180	6.06	5.0×10^{-3}

Frequency is one parameter that probably matters little in the operation of the quadrupole, except at low values. Forty-two Hertz was close to the lower limit before collisions with the electrodes took place. The focus time depends on frequency with a power of about 1/9. This is fortuitous because it implies that power line mains can be used to power a quadrupole without requiring an oscillator/power amplifier.

Although the frequency is not expected to exhibit major effects until the period approaches the relaxation time of the particle, the waveform used for the excitation may exhibit effects if portions of the waveform change abruptly (in a time short compared to the relaxation time.). Three waveform calculations are shown in Table 9, with the base case sine wave, a triangle wave, and a square wave. These are relatively easy to simulate in the model, although generating high voltages with the same characteristics may not be so easy.

Table 9. Waveform effects on focusing

Shape	Frequency (Hz)	Time to 1 % (s)	$R_{final}/R_{initial}$
Sine	60	5.65	2.9×10^{-4}
Triangle	60	8.47	4.5×10^{-3}
Square	60	2.94	1.6×10^{-7}

Here are some dramatic effects on the focusing times. The triangular waveform essentially imparts a velocity to the particle that is not far from the viscous drag limit throughout most of the cycle, except when the slope of the waveform changes. The square wave also imparts a uniform velocity near the viscous drag limit for most of the cycle, but the abrupt change of voltage

polarity induces a large departure from the viscous drag regime. This is apparently very important in the focusing process. The sine wave form is intermediate in its rates of change and their durations.

The fact that the square wave produces the same minimum time 2.94 seconds as increasing particle density does suggests that a “less than square” wave form would also produce the same results.

The azimuthal angle of the injection may show some effects, aside from collisions with the electrodes. If so, the angle of injection would have to be taken into account for purposes of determining average properties. Particle injection angles are shown in Table 10.

Table 10. Azimuthal injection angle effects on focusing

Injection angle (degrees)	Time to 1 % (s)	$R_{final}/R_{initial}$
13	6.06	5.0×10^{-4}
15	6.04	4.9×10^{-4}
30	5.84	3.8×10^{-4}
45	5.65	2.9×10^{-4}
60	5.84	3.7×10^{-4}
75	6.03	4.8×10^{-4}
77	6.05	4.9×10^{-4}

There is relatively little change of the focusing time for these injection angles. Between 0 and 13 degrees or 77 and 90 degrees, the particle trajectory would intersect the electrodes. If the initial radius of injection were reduced, the injection angle could be extended into these regions. An injection radius of 0.5 cm allows the full angular injection range to focus.

Note that there are small asymmetries in the angular injection range. This is due to the particle moving towards only one electrode at the time of release, no matter what its angular position is. It may move towards the closer electrode in one half of the angular space, but in the other half, it moves towards the same electrode that is now farther away. This is just an artifact of the model.

In the practical quadrupole, particles are injected with the electric fields having both polarities and all values of magnitude between the extremes. Mapping the full domain that results in focusing is possible but tedious. The above exercise shows that there is an injection radius for which all particles can be focused, and with approximately the same focusing time.

In summary, a working electrodynamic quadrupole shows a quadratic dependence of focusing time on both the peak ac voltage and the charge on the particles, a inverse first-order dependence of focusing time on particle density, a decided advantage for using square-wave excitation, and little dependence of focusing time on either excitation frequency or azimuthal angle of injection.

E. Implications

The concentration of 3 and 5 μm particles has been demonstrated. Very tight focusing was obtained with lower flow rates, one-half to one-fourth the maximum of 0.8 Lpm. If concentration factors are deemed important, they should scale as the ratio of cross-sectional areas occupied by the particles at the inlet and outlet of the quadrupole. The inlet cross-section is roughly 1 cm^2. If the outlet diameter is one percent of the inlet, the concentration factor would be 10^4. If the outlet beam is only one particle diameter wide, with no net force on the particles, then 5 μm particles would be concentrated by a factor of about 4.8×10^6. Smaller particles that do not focus as rapidly would not be enhanced nearly so much.

The concentration enhancement may not be as valuable for an analytic instrument as the localization would be. Confining the particles of interest to a column only a few micrometers wide means that light beams for interrogating or stimulating the particles could be focused to a much smaller volume.

Since the charged particles also repel one another, they tend to arrive at more regularly spaced time intervals in the outlet beam. This implies that the delivery rate of particles at the outlet of the quadrupole could be 2000–4000 particles per minute, roughly 35–70 per second, if we use the concentrations in Table 2. This rate could be boosted by using a higher flow rate and longer quadrupole to achieve the same focusing, assuming space charge does not become a limiting factor. State-of-the-art particle fluorescence analyzers operate at about 10 kHz (Huston, et al, 2005) and so may be slightly mismatched for this delivery rate.

Listing of all Publications and Technical Reports

Other than monthly status reports, research publications were not written due to the short duration of the project.

List of all Participating Scientific Personnel

Dr. David S. Ensor, Principal Investigator
Senior Fellow and Research Director
Center for Aerosol Technology
RTI International
Research Triangle Park, NC

Dr. Philip A. Lawless
Research Physicist
Center for Aerosol Technology
RTI International
Research Triangle Park, NC

Dr. John Franke
Professor
Department of Mathematics
NC State University
Raleigh, NC

Report of Inventions

An invention disclosure was prepared and submitted to RTI International legal council on June 16, 2006 entitled “Electrodynamic Aerosol Concentrating” by David S. Ensor and Philip A. Lawless.

Bibliography

1. Berg, T. G. O. (1970). *Method and Apparatus for Removing Particulates from Flowing Gases*. US Patent 3,496,701; February 24.

2. Biksos, G., Reavell, K., and Collings, N. "Electrostatic Characterization of Corona-wire Aerosol Chargers" *J. Electrostatics.* 63:69—82 (2005).

3. Dalley, J.E.J., Greenaway, R.S., Ulanowski, Z., Hesse, E., and Kaye, P.H. "Measurement of the Charge of Airborne 3—10 μm Spherical Dielectric Particles Charged in an ac Unipolar Charger." *J. Aerosol Sci*. 36:1194—1209 (2005).

4. Denison, D. R. (1971). Operating Parameters of a Quadrupole in a Grounded Cylindrical Housing. *J. Vac. Sci. Technol*. 8:266-269.

5. Ensor, D.S. "Development of an Electrodynamic Quadrupole Aerosol Concentrator" Final Summary Report Grant R-827354-01, by Dr. Gunther Oberdorster, Division of Respiratory Biology and Toxicology, University of Rochester Medical Center, Department of Environmental Medicine, Rochester, NY 14642 (Feb 2002).

6. Huston, A., Sivaprakasam, V., Scotto, C., Eversole, J., "Multiple Wavelength Fluorescence Excitation and Scattering for Bioaerosol Classification," Presented at 2005 Conference on Obscuration and Aerosol Research, Aberdeen, Md. (June 20-22, 2005)

7. Jaworek, A. and Krupa, A. "Airborne Particle Charging by Unipolar Ions in AC Electric Field.", *J. Electrostatics.* 23:361—370 (1989). Also, website at http://www.imp.gda.pl/ehd/chrg_aer.html

8. Keskinen, J.; Janka, K.; Lehtimäki, M. (1987). Virtual Impactor as an Accessory to Optical Particle Counters. *Aerosol Sci. Technol*. 6:79-83.

9. Kim, M. C.; Kim, D. S.; Lee, K. W.; Youn, H. J.; Choi, K. B.; Ha, Y. C. (2001). Multijet and Multistage Aerosol Concentrator: Design and Performance Analysis. *J. Aerosol Med*. 14:245-254.

10. Kim, S.; Chang, M. C.; Kim, D.; Sioutas, C. (2000). A New Generation of Portable Coarse, Fine, and Ultrafine Particle Concentrators for Use in Inhalation Toxicology. *Inhalation Toxicol*. 12:121-137.

11. Lawless, P.A. (1966) Particle Charging Bounds, Symmetry Relations, and an Analytic Charging Rate Model for the Continuum Regime." *J. Aerosol Sci*. 27:191-215.

12. Liebhaber, F. B.; Lehtimäki, M.; Willeke, K. (1991). Low-cost Virtual Impactor for Large-Particle Amplification in Optical Particle Counters. *Aerosol Sci. Technol*. 15:208-213.

13. Marple, V. A.; Chien, C. M. (1980). Virtual Impactors: a Theoretical Study. *Environ. Sci. Technol*. 14:976-985.

14. Masuda, S.; Fujibayashi, K. (1970). Electrodynamics of Charged Dust Particles Within an AC Quadrupole Electric Field: Theoretical Treatment. *Electr. Eng. Jpn.* 90:1-9.

15. Periasamy, R.; Ensor, D. S.; Donovon, R. P. (1995). *Device for Focussing Particles Suspended in a Gas Stream*. US Patent 5,439,513; August 08.

16. Romay, F. J.; Roberts, D. L.; Marple, V. A.; Liu, B. Y. H.; Olson, B. A. (2002). A High-Performance Aerosol Concentrator for Biological Agent Detection. *Aerosol Sci. Technol*. 36:217-226.

17. Sioutas, C.; Koutrakis, P.; Godleski, J. J.; Ferguson, S. T.; Kim, C. S.; Burton, R. M. (1997). Fine Particle Concentrators for Inhalation Exposures. Effect of Particle Size and Composition. *J. Aerosol Sci*. 28:1057-1071.